Falkland Islands Fisheries Department

# *Loligo* Stock Assessment, Second Season 2012

Andreas Winter

November 2012

## Index

## Summary

1) The second season *Loligo* (*D. gahi*) fishery of 2012 was open for 78 days, from July 15 to September 30. 35,026 tonnes of *D. gahi* catch were reported; the second-highest for a second season since 2004. 91% of *D. gahi* catch and 84% of effort were taken south of 52º S up to August 29, then 24% of *D. gahi* catch and 32% of effort were taken south of 52º S after August 29.
2) Sub-areas north and south of 52º S were depletion-modelled separately. In the north sub-area, two in-season depletion periods started on August 31 and September 12. A further in-season immigration started on September 26, but this was too late to depletion-model. In the south sub-area, one in-season depletion period started on August 9.
3) An estimated combined total (initial stock + in-season immigration) of 84,733 tonnes *D. gahi* (95% confidence interval: [54,420 to 275,392] tonnes) passed through the Loligo Box fishing zone during second season 2012.
4) The final total estimate for *D. gahi* remaining in the Loligo Box at the end of first season 2012 was:
   Maximum likelihood of 28,336 tonnes, with a 95% confidence interval of [14,343 to 154,807] tonnes.
   The risk of *D. gahi* escapement biomass at the end of the season being less than 10,000 tonnes was estimated at 0.37%.


## Introduction

The second season of the 2012 *Loligo* fishery (*Doryteuthis gahi* – Patagonian squid) started on July 15, and ended by directed closure on September 30. Three vessels had an extra 1-day allowance to fish on October 1 in compensation for time occupied by EU inspections, but only one vessel used the extra day for processing. Reported *D. gahi* catch by X-licensed vessels was 35,026 tonnes, the second-highest for a second season since 2004 (Table 1). Additionally 1561 tonnes *D. gahi* were caught out-of-zone north of the Loligo Box during an eight-day period. Combined with the first season, 2012 had the highest total *D. gahi* catch since 1995.

Table 1. *D. gahi* season catch comparisons since 2004.

| | Season 1 | | Season 2 | |
|---|---|---|---|---|
| | Catch (t) | Days | Catch (t) | Days |
| 2004 | | | 17,559 | 78 |
| 2005 | 24,605 | 45 | 29,659 | 78 |
| 2006 | 19,056 | 50 | 23,238 | 53 |
| 2007 | 17,229 | 50 | 24,171 | 63 |
| 2008 | 24,752 | 51 | 26,996 | 78 |
| 2009 | 12,764 | 50 | 17,836 | 59 |
| 2010 | 28,754 | 50 | 36,993 | 78 |
| 2011 | 15,271 | 50 | 18,725 | 70 |
| 2012 | 34,767 | 51 | 35,026 | 78 |

As in previous seasons, the *D. gahi* stock assessment was conducted with a depletion time-series model (Agnew et al., 1998; Roa-Ureta and Arkhipkin, 2007;

Arkhipkin et al., 2008). Because *D. gahi* has an annual life cycle (Patterson, 1988), stock cannot be derived from a standing biomass carried over from prior years (Rosenberg et al., 1990). The depletion model instead back-calculates an estimate of initial abundance from data on catch, effort, and natural mortality (Roa-Ureta and Arkhipkin, 2007). In its basic form (DeLury, 1947) the depletion model assumes a closed population in a fixed area for the duration of the assessment. This assumption is imperfectly met in the Falkland Islands fishery, where stock analyses have often shown that *D. gahi* groups arrive in successive waves after the start of the season (Roa-Ureta, 2012). Arrivals of successive groups are inferred from discontinuities in the catch data. Fishing on a single, closed cohort would be expected to yield gradually decreasing CPUE, but gradually increasing average individual sizes, as the squid grow. When instead these data change suddenly, or in contrast to expectation, the immigration of a new group to the population is indicated.

In the event of a new group arrival, the depletion calculation is modified to account for this influx. Since second season 2011, the modification has been modelled two ways: 1) by a simultaneous algorithm (Roa-Ureta, 2012) that adds new arrivals on top of the stock previously present, and assumes a common catchability coefficient for the entire depletion time-series, and 2) a sequential algorithm that re-starts the depletion time-series on the date of a new group arrival (Roa-Ureta and Arkhipkin, 2007), allowing for different catchability coefficients in the different periods of the depletion time-series. The simultaneous and sequential algorithms are shown schematically in Appendix 1 **(A.1)**. Either modelling approach may be augmented with hyper-parameters of effort and abundance. The basic form of the DeLury depletion model proposes a linear relationship of catch vs. fishing effort and abundance:

$$C_{day} = q \times E_{day} \times N_{day} \times e^{-M/2} \qquad \textbf{(1)}$$

where $C_{day}$, $E_{day}$, $N_{day}$ are catch (numbers of *D. gahi*), fishing effort, and abundance (numbers of *D. gahi*) per day, q is the catchability coefficient and M is natural mortality, considered constant at 0.0133 $day^{-1}$ (Roa-Ureta and Arkhipkin, 2007). A linear relationship means that if effort or abundance is doubled then – all else being equal – catch will double. But in reality, the relationships may depart significantly from linearity. Increases in effort are likely to elicit diminishing returns. Increases and decreases in abundance may increase or decrease relative catchability, depending on habitat conditions or the behaviour of the squid. To relate this nonlinearity in the model, the catch equation is re-defined as:

$$C_{day} = q \times E_{day}^{\alpha} \times N_{day}^{\beta} \times e^{-M/2} \qquad \textbf{(2)}$$

where α and β are respectively the effort and abundance hyper-parameters (Roa-Ureta, 2012). Advantages and disadvantages of using either the simultaneous algorithm or sequential algorithm, with or without hyper-parameters, are discussed in Winter (2012a).

Previous *D. gahi* stock assessments (e.g., Winter, 2012a, b) were calculated in a Bayesian framework whereby results of the depletion model are conditioned by prior information on the stock from the pre-season survey. In the current season, depletions did not initiate until relatively late (see 'Depletion period selection', below), and the levels of stock abundance estimated from the survey would reduce to

<40% by then, given catch and natural mortality in the meantime **(A.2)**. Additional immigration (possibly at low rates) must have occurred between the end of the survey and the start of the observed in-season depletions. Survey stock abundance estimates were therefore considered dissociated from the in-season *D. gahi* population, and not used as Bayesian priors. Likelihood of the depletion model was instead calculated directly by optimizing the difference between actual catch numbers and predicted catch numbers:

$$\sum_{days}\left(\log\left(\text{predicted } C_{day}\right)-\log\left(\text{actual } C_{day}\right)\right)^2 \qquad \textbf{(3)}$$

Distributions of the likelihood estimates (i.e., measures of their statistical uncertainty) were computed using a Markov Chain Monte Carlo (MCMC) (Gamerman and Lopes, 2006), a recommended method for fisheries assessments (Magnusson et al., 2012). MCMC is an iterative method which generates random stepwise changes to the proposed outcome of a model (in this case, the number of *D. gahi*) and at each step, accepts or nullifies the change with a probability equivalent to how well the change fits the model parameters compared to the previous step. The resulting sequence of accepted or nullified changes (i.e., the 'chain') approximates the likelihood distribution of the model outcome.

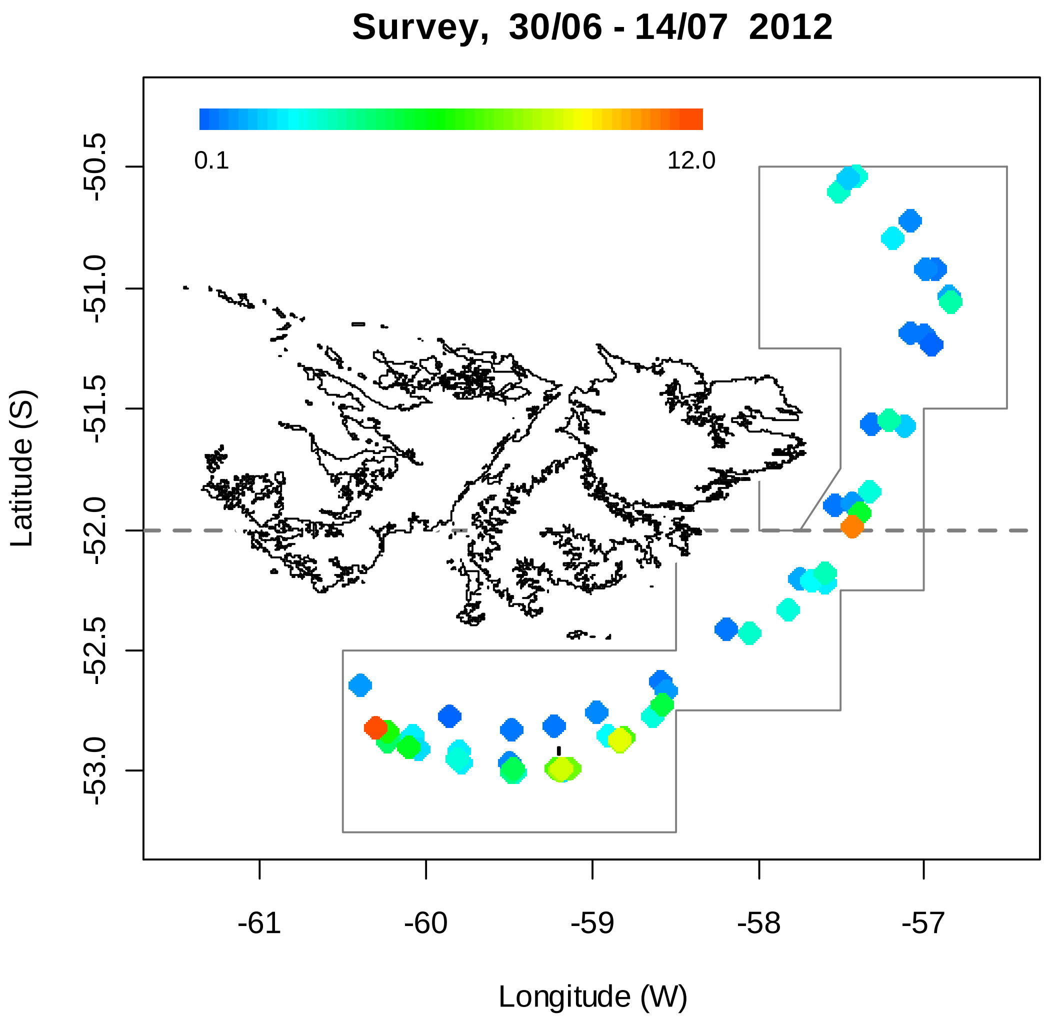

Figure 1 [previous page]. Spatial distribution of *Loligo* 2nd-season pre-season survey catches, scaled to catch weight (maximum = 12.0 tonnes). Fifty-nine catches are represented. The 'Loligo Box' fishing zone, as well as the 52 °S parallel delineating the boundary between north and south assessment sub-areas, are shown in gray.

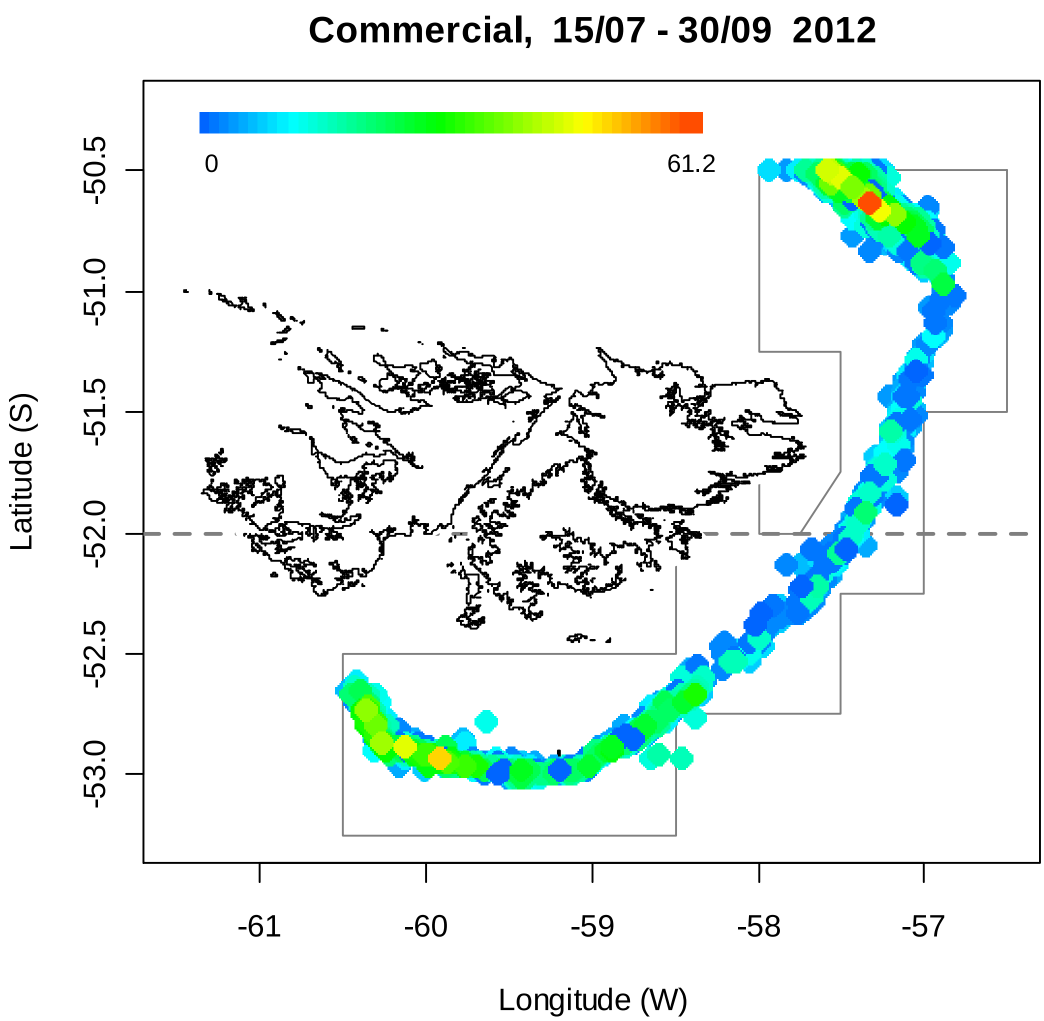


Figure 2. Spatial distribution of *Loligo* 2nd-season commercial catches, scaled to catch weight (maximum = 61.2 tonnes). 3845 catches were taken during the season. The 'Loligo Box' fishing zone, as well as the 52 °S parallel delineating the boundary between north and south assessment sub-areas, are shown in gray.

## Stock assessment
### Data

*D. gahi* catch concentrations in-season showed considerable departure from the pre-season survey. Biomass estimate from the survey was mediocre compared to other second season surveys (Winter et al., 2012), and large catches were not taken further north than 52 °S latitude, the nominal boundary between north (North-Central) and south (Beauchêne) assessment sub-areas (Figure 1). In contrast the in-season total catch was high (Table 1) and much of it came from the north end of the Loligo Box (Figure 2), and from the high seas further north. In autumn (late May) an unusual eastward extension of inner shelf waters out from the Berkeley Sound area was noted (V. Laptikhovsky and M.-J. Roux, FIFD, personal communication), suggesting higher entrainment by the Falkland Current which would result in transport of *D. gahi* recruits towards the north (Arkhipkin et al., 2006). The fishing season was largely partitioned with 84% of effort and 91% of *D. gahi* catch taken in the Beauchêne sub-area up to August 29, then after August 29 68% of effort and 76% of catch taken in the North-Central sub-area.

Between 3 and 16 vessels fished in the commercial season on any day (median = 15; Figure 3), for a total of 1094 vessel-days. These vessels reported daily catch totals to the FIFD and electronic logbook data that included trawl times, positions, and product weight by market size categories.

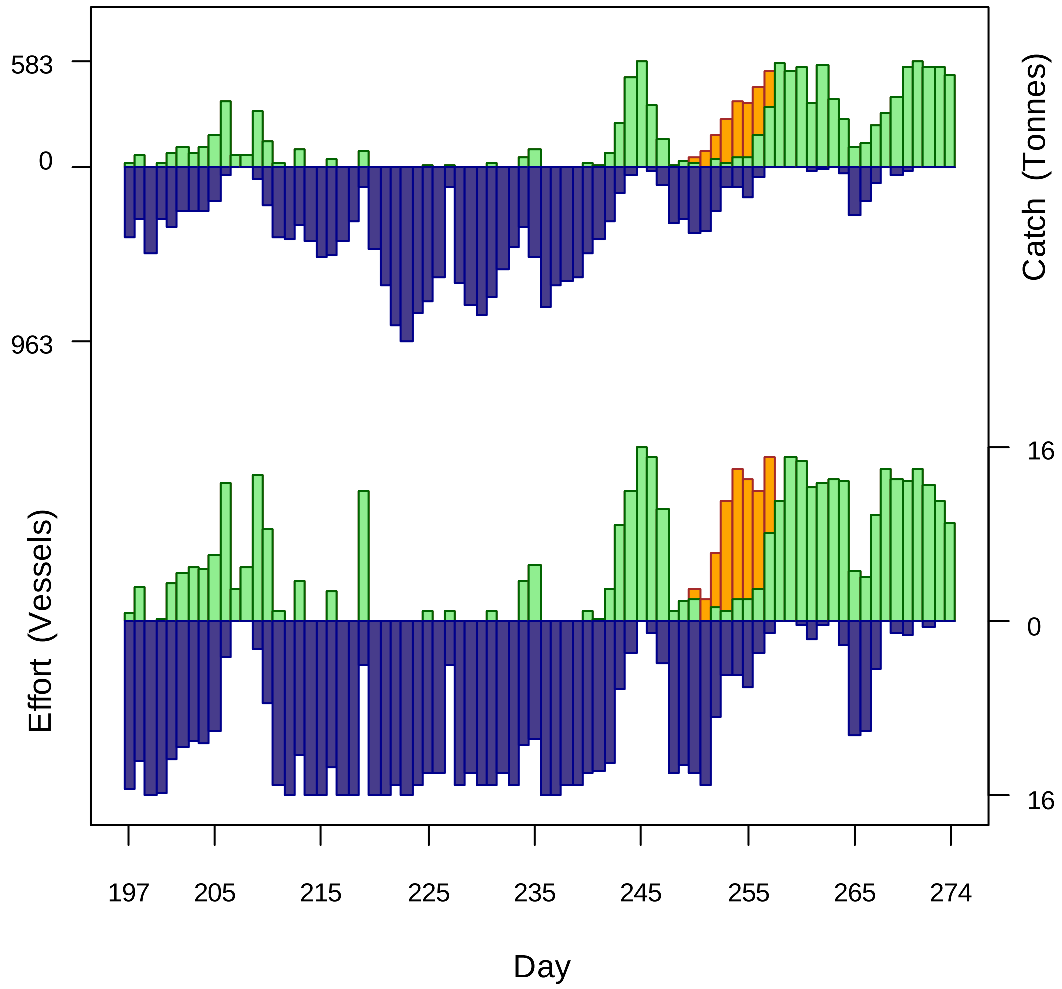


Figure 3. Daily total *D. gahi* catch and effort distribution by assessment sub-area north (green) and south (purple) of the 52º S parallel in the *Loligo* 2nd season 2012, plus catch and effort taken out-of-zone further north (orange). The season was open from July 15 (chronological day 197) to September 30 (chronological day 274). As many as 16 vessels fished per day north of 52º S; as many as 16 vessels fished per day south of 52º S. As much as 583 tonnes *D. gahi* were caught per day north of 52º S; as much as 963 tonnes *D. gahi* were caught per day south of 52º S.

Three FIFD observers were deployed on three vessels in the fishery for a total of 77 observer-days. Throughout the 78 days of the season, 3 days had no observer covering, 73 days had 1 observer covering, and 2 days had two observers covering. Each observer sampled an average of 413 *D. gahi* daily, and reported their maturity stages, sex, and lengths to 0.5 cm.

**Group arrivals / depletion criteria**

Start and end days of depletions - following arrivals of new *D. gahi* groups - were judged with reference to daily changes in CPUE, sex ratios, maturity, and average individual sizes. CPUE was calculated as metric tonnes of *D. gahi* caught per vessel per day. Days were used rather than trawl hours as the basic unit of effort. Commercial vessels do not trawl standardized duration hours, but rather durations that best suit their daily processing requirements. An effort index of days is therefore more consistent. Daily average individual *D. gahi* sizes were expressed as weight (kg), converted from mantle lengths using Roa-Ureta and Arkhipkin's (2007) formula optimized on length-weight data from the pre-season survey (Winter et al., 2012):

$$\text{weight (kg)} = 0.2780914 \times \mathit{length}\ (\mathit{cm})^{1.9987736} / 1000 \qquad \textbf{(4)}$$

For the daily average individual sizes, mantle lengths were obtained from in-season observer data, and also derived from in-season commercial data as the proportion of product weight that vessels reported per market size category. Observer mantle lengths are scientifically precise, but restricted to 1-2 vessels at any one time that may or may not be representative of the entire fleet. Commercially proportioned mantle lengths are relatively imprecise, but cover the entire fishing fleet. Therefore, both sources of data were used. Daily average individual weights were calculated by averaging observer size samples and commercial size categories where observer data were available, otherwise only commercial size categories.

**Depletion period selection**

With the large-scale partition in the fishing season, sub-areas north and south of 52ºS were depletion-modelled separately. The *D. gahi* data and CPUE time series showed two days in the north and one day in the south that plausibly represent the onset of separate depletions. Additionally the data indicate that an immigration occurred north near the end of the season (Figures 4 and 5), but this could no longer be depletion-modelled.

- The first in-season depletion north was identified on day 244 (31 August), with a strong increase in CPUE (Figure 4), coincident with a peak in average commercial weight (Figure 5, top graph). Average observed weights were available in the north following day 244, and showed a brief decrease trend, consistent with the commercial weight data (Figure 5, 2nd graph).
- The second in-season depletion north was identified on day 256 (12 September), again with a strong increase in CPUE (Figure 4), a peak in average commercial weight (Figure 5, top graph), and a following decrease trend in average observed weight (Figure 5, 2nd graph). Observer data also showed an increased trend in female proportion after day 256 (Figure 5, 3rd graph).

- The additional late-season immigration in the northern sub-area was identified on day 270 (26 September) with a strong increase in CPUE (Figure 4) and a local minimum in average commercial weight (Figure 5, top graph).
- The single in-season depletion south was identified on day 222 (9 August) with a strong increase in CPUE (Figure 4). Observer data suggest that around this day the female proportion increased slightly within an overall decreasing trend (Figure 5, 3rd graph).

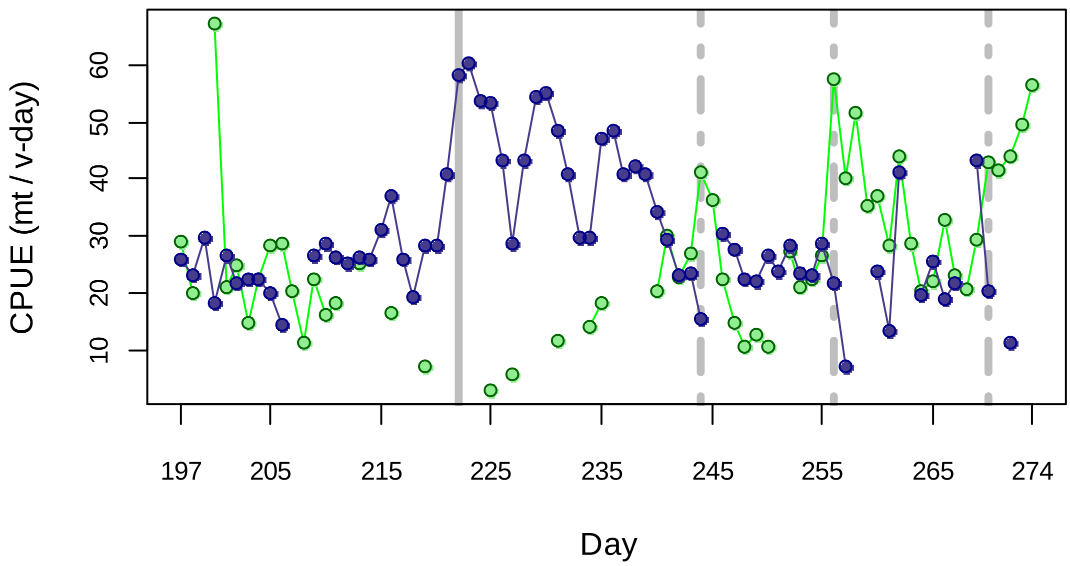


Figure 4. CPUE in metric tonnes per vessel per day, by assessment sub-area north (green) and south (purple) of the 52º S parallel. Data from consecutive days are joined by line segments. Broken gray vertical bars indicate days 244, 256, and 270, identified as the start of in-season depletion or immigration north. Solid gray vertical bar indicates day 222, identified as the start of in-season depletion south.

## Depletion models

Four versions of the depletion model were tested by optimizing equation **(3)**: the simultaneous model with hyper-parameters (A), the simultaneous model without hyper-parameters (B), and the sequential model with (C) and without (D) hyper-parameters. An additional variant for each version ($A_w$, $B_w$, $C_w$, $D_w$) was tested by weighting the daily catches ($C_{n\ day}$ in equation **(3)**) as a function of the daily effort (number of vessels fishing). This was done because the level of effort throughout a depletion period was in some cases very uneven (Figure 3), incurring the possibility that optimizations could be skewed by days that in reality had little fishing activity.

Comparative results are shown in **(A.3)**. Weighted model versions were found to provide insufficient advantage: improvements in root mean square error RMSE were in most cases marginal, if at all. Among unweighted model versions, for sub-area north: Version A was eliminated because the end abundance N of 0.04 billion was unrealistically low. Version C was eliminated because the abundance hyper-parameter was unrealistically high and the difference in q between the first and second depletion was unrealistically high. Version D was eliminated because the

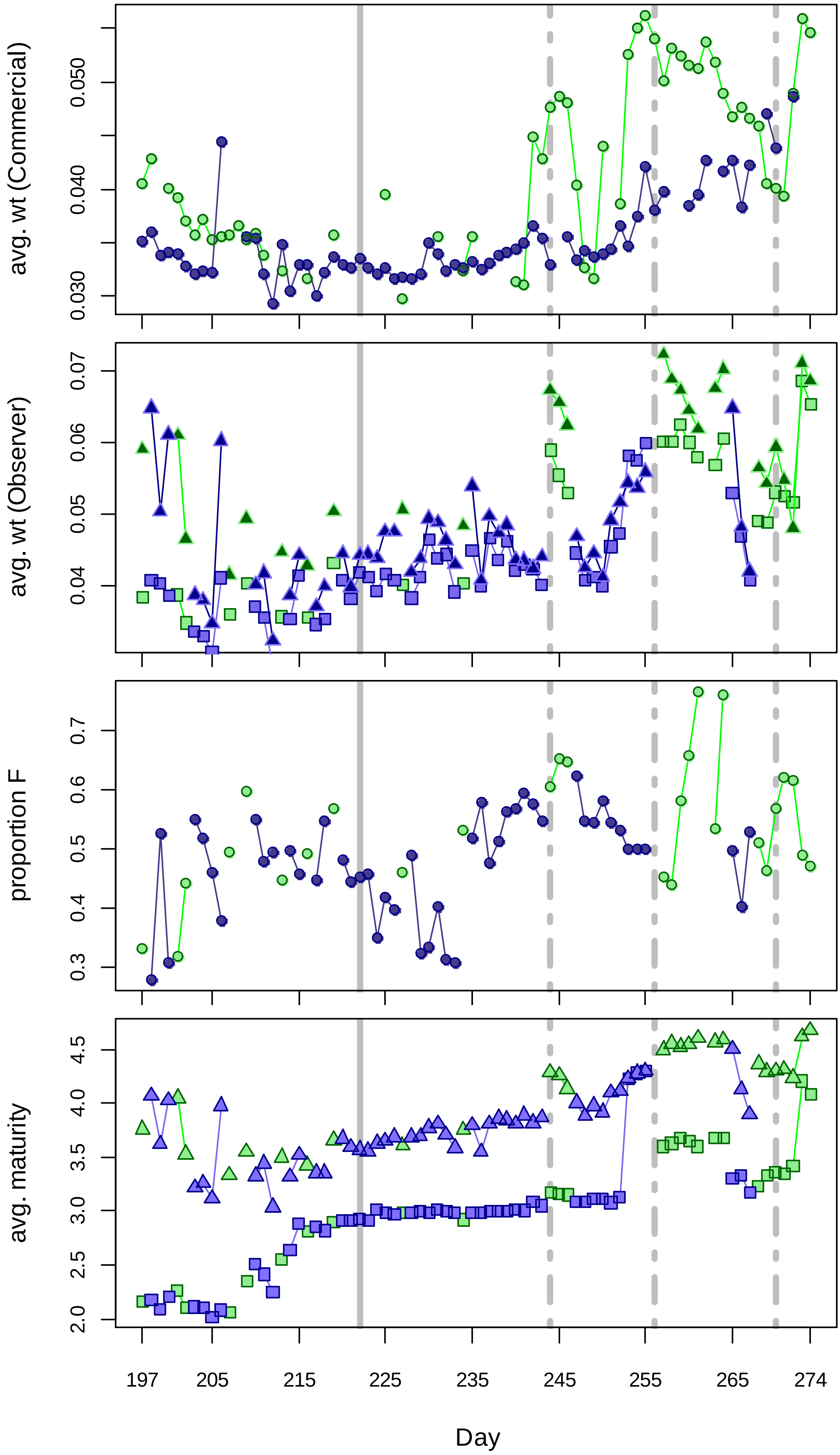
avg. wt (Commercial)
0.030
0.040
0.050
avg. wt (Observer)
0.04
0.05
0.06
0.07
proportion F
0.3
0.4
0.5
0.6
0.7
avg. maturity
2.0
2.5
3.0
3.5
4.0
4.5
197
205
215
225
235
245
255
265
274
Day

Figure 5 [Previous page]. Top graph: Average individual *D. gahi* weights (kg) per day from commercial size categories. 2nd graph: Average individual *D. gahi* weights (kg) by sex per day from observer sampling. 3rd graph: Proportions of female *D. gahi* per day from observer sampling. Bottom graph: avg. maturity value by sex per day from observer sampling. Males: triangles, females: squares, unsexed: circles. North sub-area: green, south sub-area: purple. Data from consecutive days are joined by line segments. Broken gray vertical bars indicate days 244, 256, and 270, identified as the start of in-season depletion or immigration north. Solid gray vertical bar indicates day 222, identified as the start of in-season depletion south.

abundance N of the first depletion was too low and the difference in q between the first and second depletion was unrealistically high. That left version B. For sub-area south: Version D was not preferred because the q was relatively low and the end abundance N was relatively high (less conservative). That left C (versions A and B don't pertain in the south because only one depletion period was identified). Version B in the north and C in the south showed reasonably similar q values (less than 2× difference), and were therefore retained as the appropriate models in either sub-area.

The MCMC of the models were run for 500,000 iterations; the first 1000 iterations were discarded as burn-in sections (initial phases over which the algorithm stabilizes); and the chains were thinned by a factor of 10 to reduce serial correlation (only every tenth iteration was retained). For each model (B – north and C – south) nine chains were run; one chain initiated with the optimized parameter values from equation (3) (as shown in Table **A.3**), then eight chains with different combinations of high (2×) and low (¼×) parameter values.

## Depletion analyses

### *North*

The simultaneous model with two depletion periods and no hyper-parameters required an expansion of equation **(1)**:

$$C_{day} = q \times E_{day} \times (N1_{day} + (N2_{day} \times i2\big|_0^1)) \times e^{-M/2} \qquad \textbf{(5)}$$

(Roa-Ureta, 2011), where i2 is a dummy variable taking the values 0 or 1 if 'day' is before or after the start day of the second depletion. The model optimized for q, N1, and N2.

MCMC revealed that this depletion model stabilized in two alternate states: low catchability coefficient q with corresponding high N values, and high q with low N (Figure 6). N1 values (N at the start of the first depletion) corresponding to the low q state reached 3-4 billion *D. gahi*, which would have been equivalent to a biomass of 123,000 – 164,000 tonnes. This is unrealistic, and the low q state was therefore considered a spurious optimization. Parameters corresponding to $q \leq 0.0005$ (see horizontal line through the top graph of Figure 6) were excluded from calculating the variability distribution of the stock.

Because a new immigration was inferred on day 270, depletion was only modelled to day 269. *D. gahi* numbers on day 269 were calculated as the numbers N1 and N2 on depletion start days 244 and 256, discounted for natural mortality during the intervening period, and subtracting cumulative catch also discounted for natural mortality (CNMD):

$$\text{CNMD}_{\text{day } 0} = 0$$

$$\text{CNMD}_{\text{day } x} = \text{CNMD}_{\text{day x-1}} \times e^{-M} + C_{\text{day x-1}} \times e^{-M/2} \quad \textbf{(6)}$$

$$\begin{aligned} N_{\text{N day 269}} &= N1_{\text{N day 244}} \times e^{-M(269-244)} + N2_{\text{N day 256}} \times e^{-M(269-256)} \\ &\quad - \text{CNMD}_{\text{N day 269}} \\ &= 0.201 \times 10^{9} \end{aligned} \quad \textbf{(7)}$$

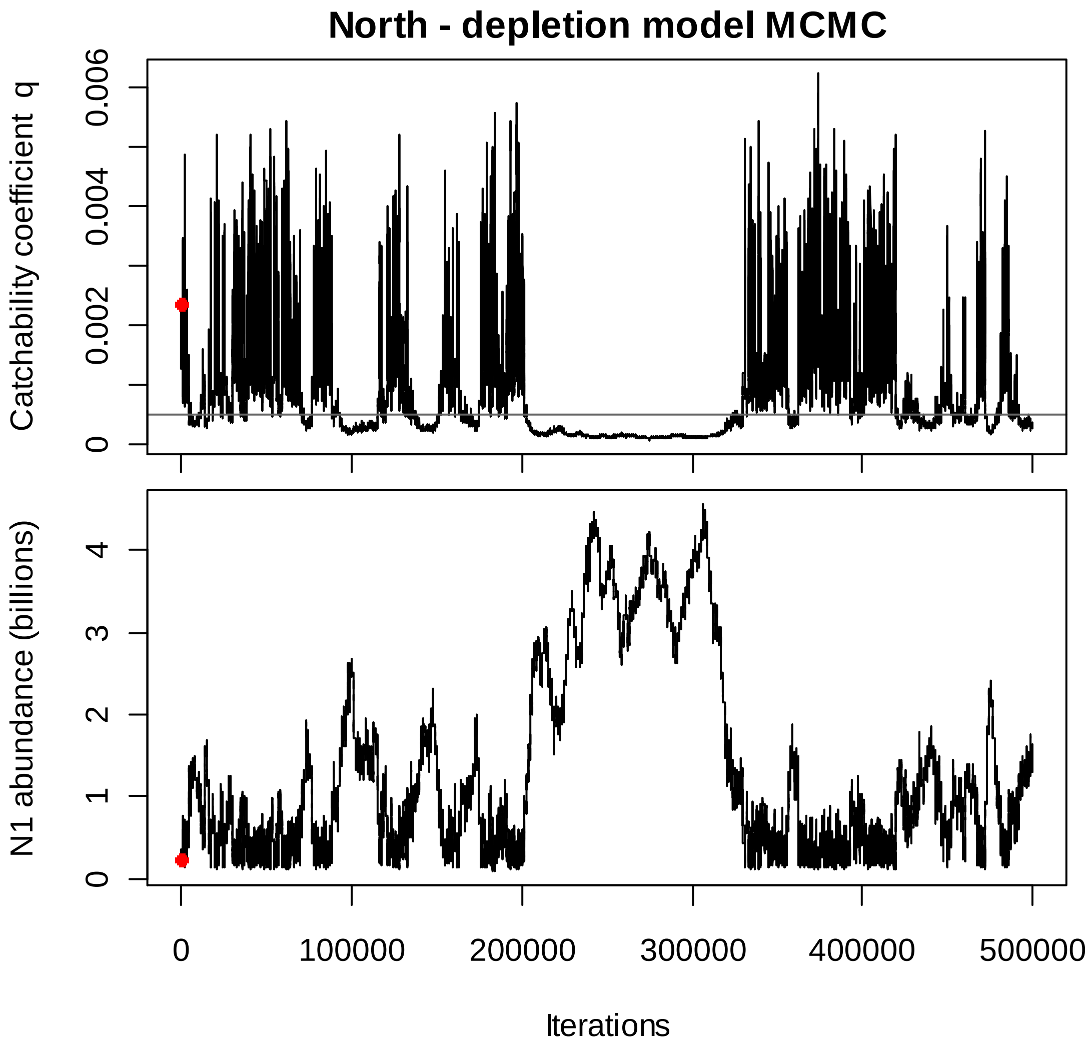


Figure 6. MCMC iteration from the north sub-area depletion model, showing the two alternating 'states' of low or high catchability coefficient q (top graph), with corresponding high or low N1 abundance (bottom graph). Horizontal gray line on the top graph shows the q = 0.0005 threshold line used to reject the low q state. Red dots on both graphs indicate the respective optimized values.

Biomass on day 269 was calculated as abundance N× individual *D. gahi* weight **(A.4)**:

$$\begin{aligned} B_{\text{N day 269}} &= N_{\text{N day 269}} \times Wt_{\text{N day 269}} = 0.201 \times 10^{9} \times 51.3 \text{ g} \\ &= 10{,}283 \text{ tonnes} \end{aligned} \quad \textbf{(8)}$$

This biomass was extrapolated to the final day of the season (day 274) by applying the equivalence of $B_{N\ day\ 274} / B_{N\ day\ 269} = C_{N\ day\ 274} / C_{N\ day\ 269}$. The ratio of catch rather than CPUE was used because on the last day or two of the season vessels will tend to fish as much as they can hold, whereas earlier in the season they will tend to fish only as much as they can process within ~24 hours. Therefore total catch is likely to be a less biased representation of the amount of *D. gahi* available. Estimated biomass on the final day of the season was then:

$$
\begin{aligned}
B_{N\ day\ 274} &= B_{N\ day\ 269} \times C_{N\ day\ 274} / C_{N\ day\ 269} \\
&= 10{,}283 \text{ tonnes} \times 507.9 / 381.9 \\
&= 13{,}678 \text{ tonnes} \qquad \textbf{(9)}
\end{aligned}
$$

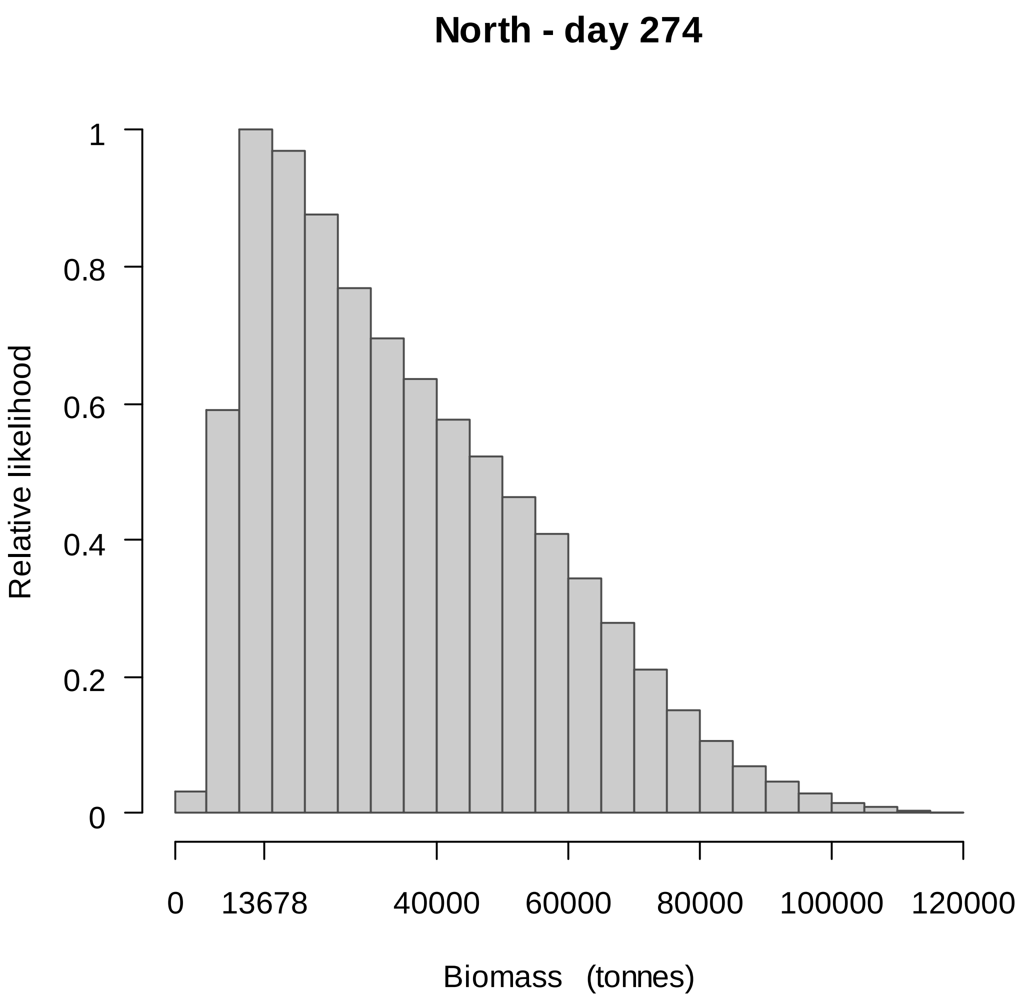


Figure 7. Likelihood distribution of *D. gahi* biomass in the north sub-area, day 274 (Sept. 30).

The likelihood distribution for $B_{N\ day\ 274}$ was calculated by repeating the sequence of equations **(7, 8, 9)** with $N1_{N\ day\ 244}$ and $N2_{N\ day\ 256}$ substituted by values drawn from the MCMC, $Wt_{N\ day\ 269}$ substituted by values randomly drawn from the normal distribution (mean = $Wt_{N\ day\ 269}$, standard deviation calculated from the GAM fit,

**A.4**), and $C_{N\ day\ 274}$ and $C_{N\ day\ 269}$ substituted by random bootstrap draws with replacement among the catch totals of vessels fishing on either day. The process was repeated 596,874×; 6× the number of MCMC iterations retained after thresholding for q > 0.0005. The distribution is strongly positive-skewed (Figure 7), and corresponds to a 95% confidence interval of [7382 – 82,716] tonnes.

***South***

The model of one single depletion period with hyper-parameters was equivalent to equation (2); optimizing for q, N, α, and β. MCMC again revealed that the depletion model stabilized in two alternate states: low q with high N values, and high q with low N (Figure 8). The low q state was rejected (corresponding N values were unrealistically as high as 9 billion *D. gahi*, equivalent to approx. 329,000 tonnes), with a threshold set at q > 0.0002 (horizontal line through the top graph of Figure 8).

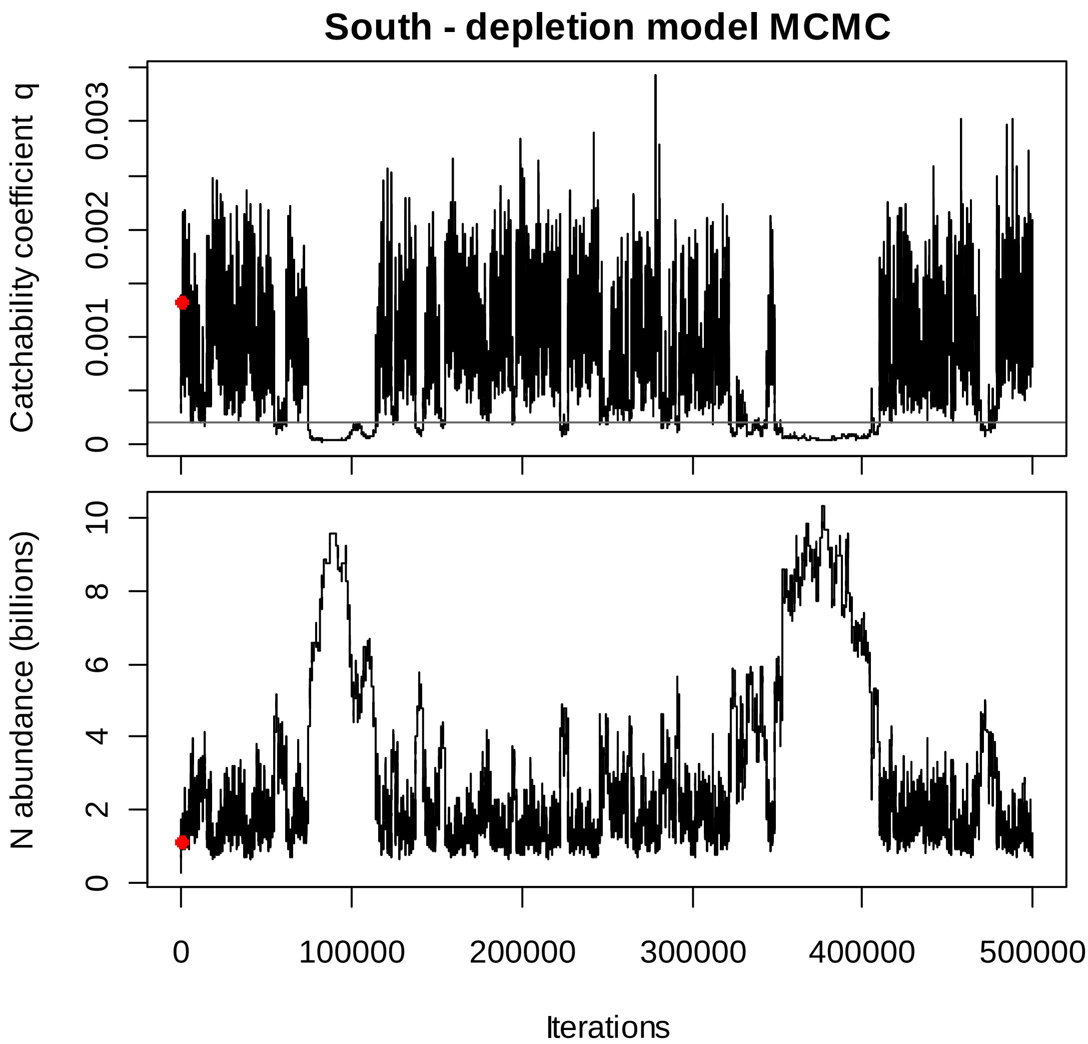


Figure 8. MCMC iteration from the south sub-area depletion model, showing the two alternating ‘states’ of low or high catchability coefficient q (top), with corresponding high or low N abundance (bottom). Horizontal gray line on the top graph shows the q = 0.0002 threshold line used to reject the low q state. Red dots indicate the respective optimized values.

The depletion was modelled from day 222 through day 270, the last full day of fishing in the south by at least one vessel (Figure 3). Unlike the north however, no resurgence of CPUE occurred after day 270, and therefore the depletion was extrapolated through to the end of the season.

$$N_{S\ day\ 274} = N_{S\ day\ 222} \times e^{-M(274-222)} - CNMD_{S\ day\ 274} = 0.320 \times 10^9 \quad \textbf{(10)}$$

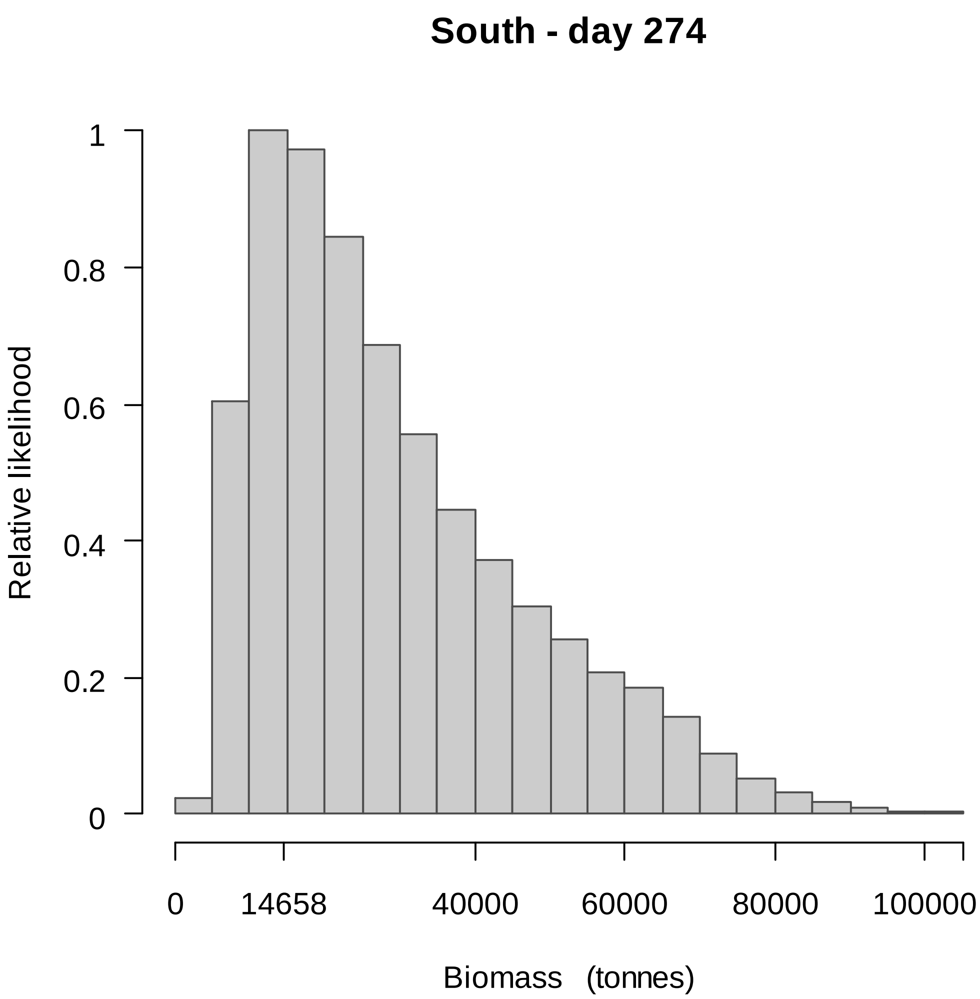


Figure 9. Likelihood distribution of *D. gahi* biomass in the south sub-area, day 274 (Sept. 30).

Biomass on day 274 was calculated as abundance N× individual *D. gahi* weight **(A.4)**:

$$B_{S\ day\ 274} = N_{S\ day\ 274} \times Wt_{S\ day\ 274} = 0.320 \times 10^9 \times 45.8\ g = 14{,}658\ tonnes \quad \textbf{(11)}$$

The likelihood distribution for $B_{S\ day\ 274}$ was calculated by repeating equations **(10)** and **(11)** with $N_{S\ day\ 222}$ substituted by values drawn from the MCMC, and $Wt_{S\ day\ 274}$ substituted by values randomly drawn from the normal distribution (mean = $Wt_{S\ day}$

$_{274}$, standard deviation calculated from the GAM fit, **A.4**). The process was repeated 689,870×; 2× the number of MCMC iterations retained after thresholding for q > 0.0005. The distribution is also positive-skewed (Figure 9), and corresponds to a 95% confidence interval of [6965 – 72,097] tonnes.

**Immigration and aggregate biomass**

*D. gahi* immigration N (after the start of the season) was inferred as the difference between the N maximum likelihood estimate on each depletion start day (when the immigrations putatively occurred) and the predicted number on that day that would be accounted for by depletion of the previous population alone. This immigration number was then multiplied by the average individual weight to give biomass.

For the first depletion north (day 244), immigration was (details in **A.5**):

$$N_{\text{N immigration day 244}} = N1_{\text{N day 244}} - N_{\text{N survey day 244}}$$
$$= (0.224 - 0.093) \times 10^9$$
$$= 0.132 \times 10^9 \sim \text{95\% CI } [0.044 - 0.914] \times 10^9$$
$$B_{\text{N immigration day 244}} = 5406 \sim \text{95\% CI } [1812 - 37{,}764] \text{ tonnes} \quad \textbf{(12)}$$

For the second depletion north (day 256), immigration was (**A.5**):

$$N_{\text{N immigration day 256}} = N2_{\text{N day 256}} \quad \text{(because the model was simultaneous)}$$
$$= 0.167 \times 10^9 \sim \text{95\% CI } [0.117 - 0.636] \times 10^9$$
$$B_{\text{N immigration day 256}} = 8736 \sim \text{95\% CI } [6099 - 33{,}420] \text{ tonnes} \quad \textbf{(13)}$$

The third immigration north (day 270) was inferred as the difference between the abundance estimated by depletion and the abundance estimated by catch ratio (**A.5**):

$$N_{\text{N immigration day 270}} = N_{\text{N day 270 ratio}} - N_{\text{N day 270 depletion}}, \text{ where}$$
$$N_{\text{N day 270 ratio}} = N_{\text{N day 269}} \times C_{\text{N day 270}} / C_{\text{N day 269}}$$
$$N_{\text{N day 270 depletion}} = N1_{\text{N day 244}} \times e^{-M(270-244)} + N2_{\text{N day 256}} \times e^{-M(270-256)} - CNMD_{\text{N day 270}}$$
$$N_{\text{N immigration day 270}} = 0.099 \times 10^9 \sim \text{95\% CI } [0.018 - 0.733] \times 10^9$$
$$B_{\text{N immigration day 270}} = 5076 \sim \text{95\% CI } [942 - 37{,}774] \text{ tonnes} \quad \textbf{(14)}$$

For the depletion south (day 222), immigration was (**A.5**):

$$N_{\text{S immigration day 222}} = N_{\text{S day 222}} - N_{\text{S survey day 222}}$$
$$= (1.133 - 0.134) \times 10^9$$
$$= 0.999 \times 10^9 \sim \text{95\% CI } [0.654 - 3.500] \times 10^9$$
$$B_{\text{S immigration day 222}} = 36{,}516 \sim \text{95\% CI } [23{,}874 - 128{,}027] \text{ tonnes} \quad \textbf{(15)}$$

The estimated total in-season immigration biomass was:

$$B_{\text{immigration total}} = 5406 + 8736 + 5076 + 36{,}516$$
$$= 55{,}735 \sim \text{95\% CI } [32{,}709 - 236{,}992] \text{ tonnes} \quad \textbf{(16)}$$

The estimated aggregate biomass (initial + immigration) to have passed through the Loligo Box fishery zone in the second season of 2012 was (**A.2** and **A.5**):

$$B_{\text{season total}} = B_{\text{N survey}} + B_{\text{S survey}} + B_{\text{immigration total}}$$

$$= 84{,}733 \sim 95\%\ \text{CI}\ [54{,}420 - 275{,}392]\ \text{tonnes} \qquad \textbf{(17)}$$

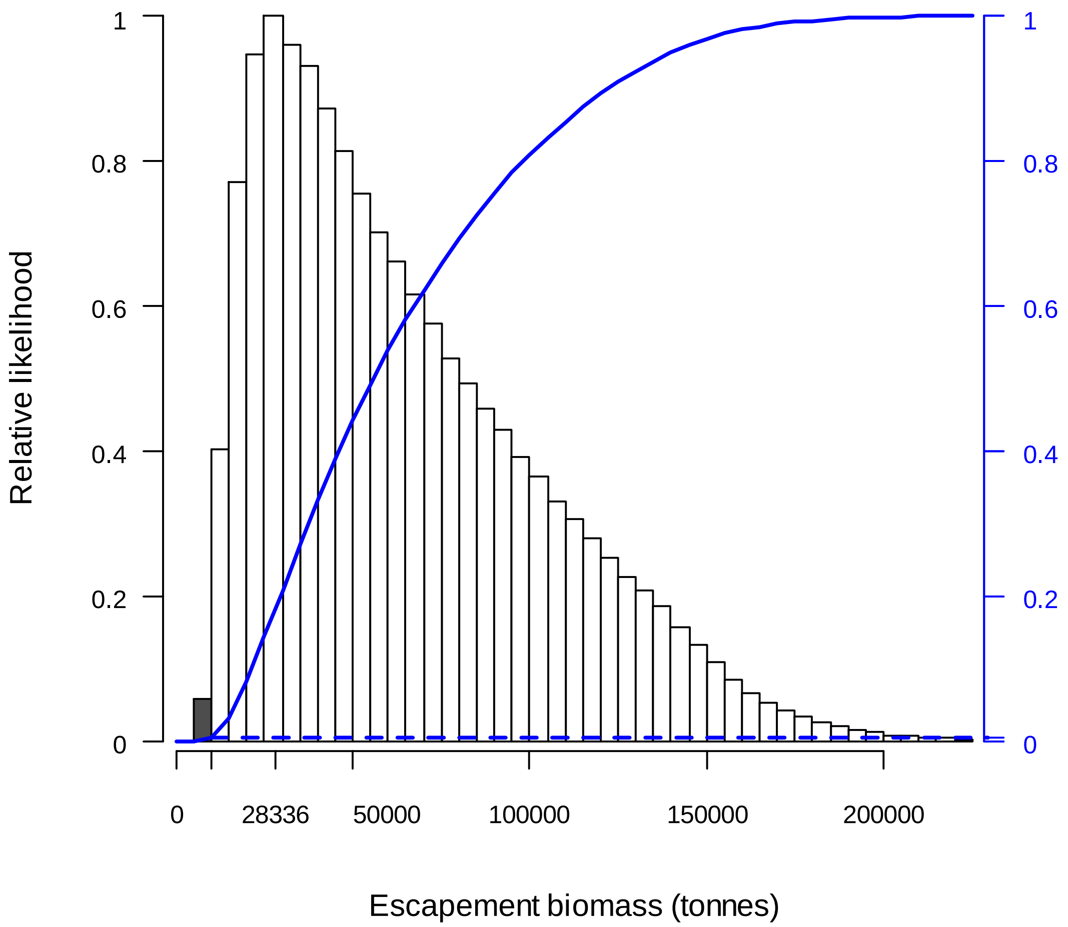


Figure 10. Likelihood distribution of *D. gahi* biomass at the end of the season, September 30. Distribution outcomes less than the biomass escapement limit of 10,000 tonnes are shaded dark gray. Cumulative likelihood is shown as a solid blue curve. The broken blue line indicates the cumulative likelihood of less than 10,000 tonnes escapement biomass: 0.37%.

## Escapement biomass

Escapement biomass was defined as the aggregate biomass of *D. gahi* at the end of the season (day 274; September 30) for the north and south sub-areas combined (equations **9** + **11**):

$$B_{\text{Total day 274}} = B_{\text{N day 274}} + B_{\text{S day 274}}$$

$= 28{,}336 \sim 95\%\ CI\ [14{,}343 – 154{,}807]$ tonnes

The likelihood distribution of the escapement biomass is shown in Figure 10. The risk of the fishery, defined as the proportion of the escapement biomass distribution below the conservation limit of 10,000 tonnes (Agnew et al., 2002; Barton, 2002), was equal to 0.37%.

## References


Agnew, D.J., Baranowski, R., Beddington, J.R., des Clers, S., Nolan, C.P. 1998. Approaches to assessing stocks of *Loligo gahi* around the Falkland Islands. Fisheries Research 35:155-169.

Agnew, D. J., Beddington, J. R., and Hill, S. 2002. The potential use of environmental information to manage squid stocks. Canadian Journal of Fisheries and Aquatic Sciences, 59: 1851–1857.

Arkhipkin, A.I., Laptikhovsky, V.V., Sirota, A.M., Grzebielec, R. 2006. The role of the Falkland Current in the dispersal of the squid *Loligo gahi* along the Patagonian Shelf. Estuarine, Coastal, and Shelf Science 67:198-204.

Arkhipkin, A.I., Middleton, D.A.J., Barton, J. 2008. Management and conservation of a short-lived fishery resource: *Loligo gahi* around the Falkland Islands. American Fisheries Society Symposium 49:1243-1252.

Barton, J. 2002. Fisheries and fisheries management in Falkland Islands Conservation Zones. Aquatic Conservation: Marine and Freshwater Ecosystems, 12: 127–135.

DeLury, D.B. 1947. On the estimation of biological populations. Biometrics 3:145-167.

Gamerman, D., Lopes, H.F. 2006. Markov Chain Monte Carlo. Stochastic simulation for Bayesian inference. 2nd edition. Chapman & Hall/CRC.

Magnusson, A., Punt, A., Hilborn, R. 2012. Measuring uncertainty in fisheries stock assessment: the delta method, bootstrap, and MCMC. Fish and Fisheries DOI: 10.1111/j.1467-2979.2012.00473.x

Patterson, K.R. 1988. Life history of Patagonian squid *Loligo gahi* and growth parameter estimates using least-squares fits to linear and von Bertalanffy models. Marine Ecology Progress Series 47:65-74.

Roa-Ureta, R.H. 2011. CatDyn: Fishery Stock Assessment by Catch Dynamic Models. R package version 1.0-3.

Roa-Ureta, R. 2012. Modelling in-season pulses of recruitment and hyperstability-hyperdepletion in the *Loligo gahi* fishery around the Falkland Islands with generalized depletion models. ICES Journal of Marine Science, 69: 1403–1415.

Roa-Ureta, R., Arkhipkin, A.I. 2007. Short-term stock assessment of *Loligo gahi* at the Falkland Islands: sequential use of stochastic biomass projection and stock depletion models. ICES Journal of Marine Science 64:3-17.

Rosenberg, A.A., Kirkwood, G.P., Crombie, J.A., Beddington, J.R. 1990. The assessment of stocks of annual squid species. Fisheries Research 8:335-350.

Winter, A. 2012a. *Loligo gahi* stock assessment, second season 2011. Technical Document, Falkland Islands Fisheries Department.

Winter, A. 2012b. *Loligo gahi* stock assessment, first season 2012. Technical Document, Falkland Islands Fisheries Department.

Winter, A., Shcherbich, Z., Hancox, E. 2012. *Loligo* stock assessment survey, second season 2012. Technical Document, Falkland Islands Fisheries Department.

**Appendix**

**(A.1)** Schematic comparison of simultaneous and sequential depletion models.

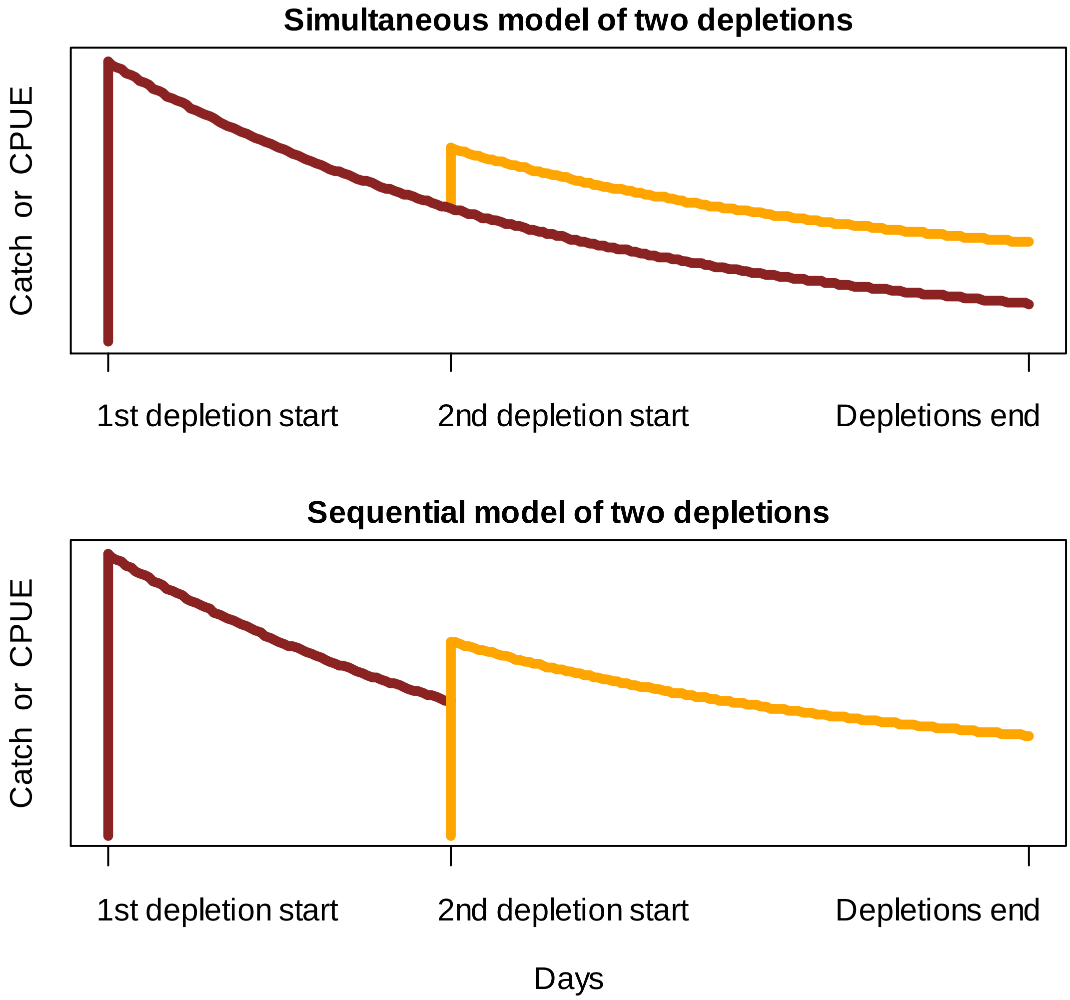


Figure A.1. Schematic of the difference between simultaneous depletion modelling (Roa-Ureta, 2012) and sequential depletion modelling (Roa-Ureta and Arkhipkin, 2007). In the simultaneous model numbers of *D. gahi* from the two depletion curves must be added together on any day; in the sequential model the second depletion curve includes the numbers from the first one.

**(A.2)** *D. gahi* abundance estimation from the survey.

The pre-season survey estimated *D. gahi* biomass at 10,838 tonnes ± 37.7% north of 52°S and 18,160 tonnes ± 36.1% south of 52°S (Winter et al., 2012). *D. gahi* were sampled at 59 pre-season survey stations, giving weighted average mantle lengths (both sexes) of 12.50 cm ± 12.6% north and 12.16 cm ± 9.1% south, corresponding to 0.043 and 0.041 kg individual weight. Survey estimate numbers are thus:

$$
\begin{aligned}
N_{N\ survey} &= 10838\ t / 0.043\ kg = 0.250 \times 10^9 \pm \sqrt{37.7\%^2 + 12.6\%^2} \\
&= 0.250 \times 10^9 \pm 39.7\% \\
&= 0.250 \pm 0.099 \times 10^9 \\
N_{S\ survey} &= 18160\ t / 0.041\ kg = 0.443 \times 10^9 \pm \sqrt{36.1\%^2 + 9.1\%^2} \\
&= 0.443 \times 10^9 \pm 37.3\% \\
&= 0.443 \pm 0.165 \times 10^9
\end{aligned}
$$

By the start of the first depletion periods (day 244 north and day 222 south), these numbers would be reduced by catch and natural mortality as:

$$
\begin{aligned}
N_{N\ survey\ day\ 244} &= N_{N\ survey} \times e^{-M(244-197)} - CNMD_{N\ day\ 244} \\
&= 0.093 \times 10^9 \pm 39.7\% \\
&= 0.093 \pm 0.037 \times 10^9
\end{aligned}
$$

$$
\begin{aligned}
N_{S\ survey\ day\ 222} &= N_{S\ survey} \times e^{-M(222-197)} - CNMD_{S\ day\ 222} \\
&= 0.134 \times 10^9 \pm 37.3\% \\
&= 0.134 \pm 0.050 \times 10^9
\end{aligned}
$$

The proportional reductions are:

$$
\begin{aligned}
N_{N\ survey\ day\ 244} / N_{N\ survey} &= 0.093 / 0.250 = 37.0\% \\
N_{S\ survey\ day\ 222} / N_{S\ survey} &= 0.134 / 0.443 = 30.2\%
\end{aligned}
$$

**(A.3)** Evaluation of different versions of the depletion model.

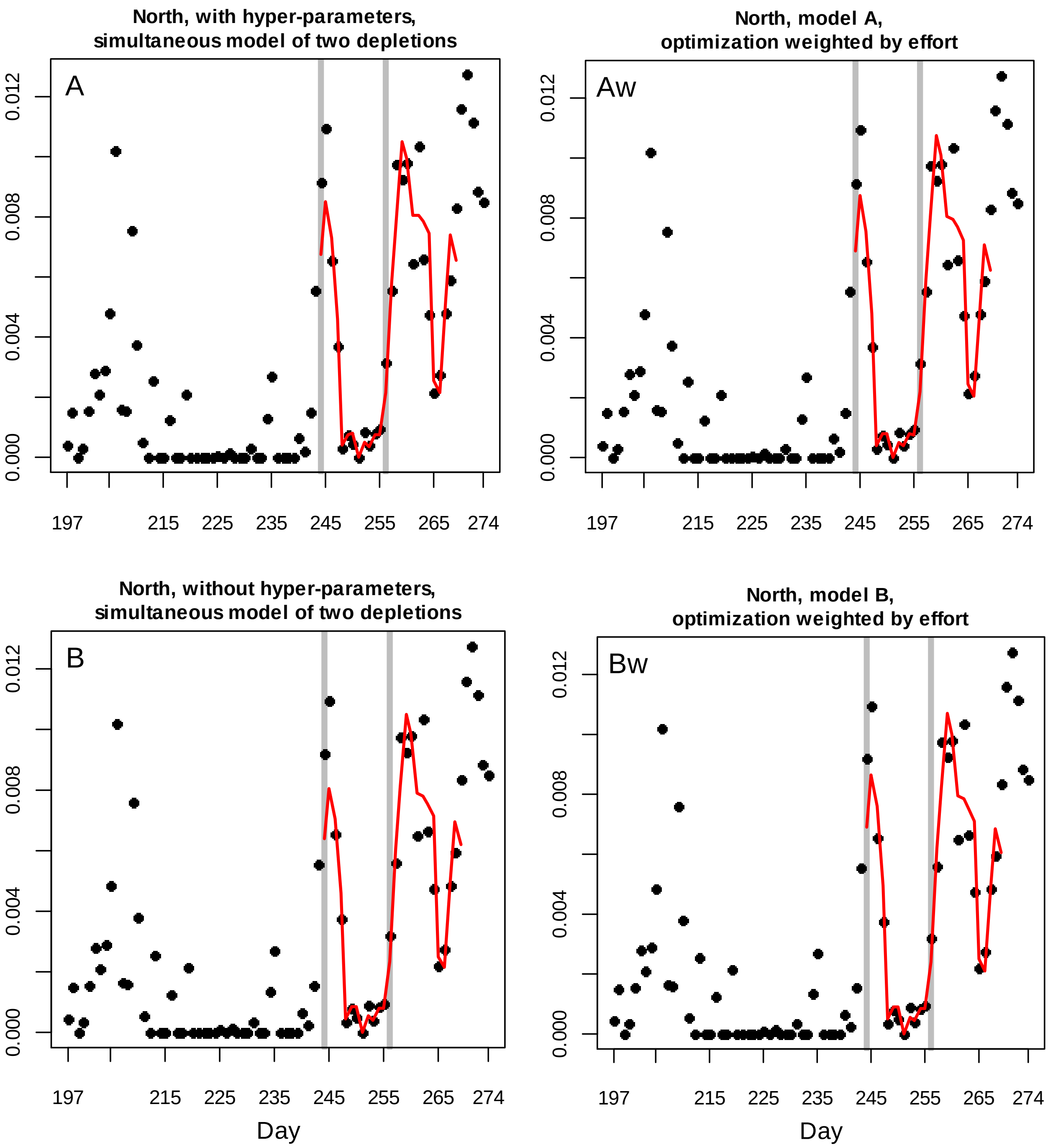


Figure A.3.1. (Continued below).

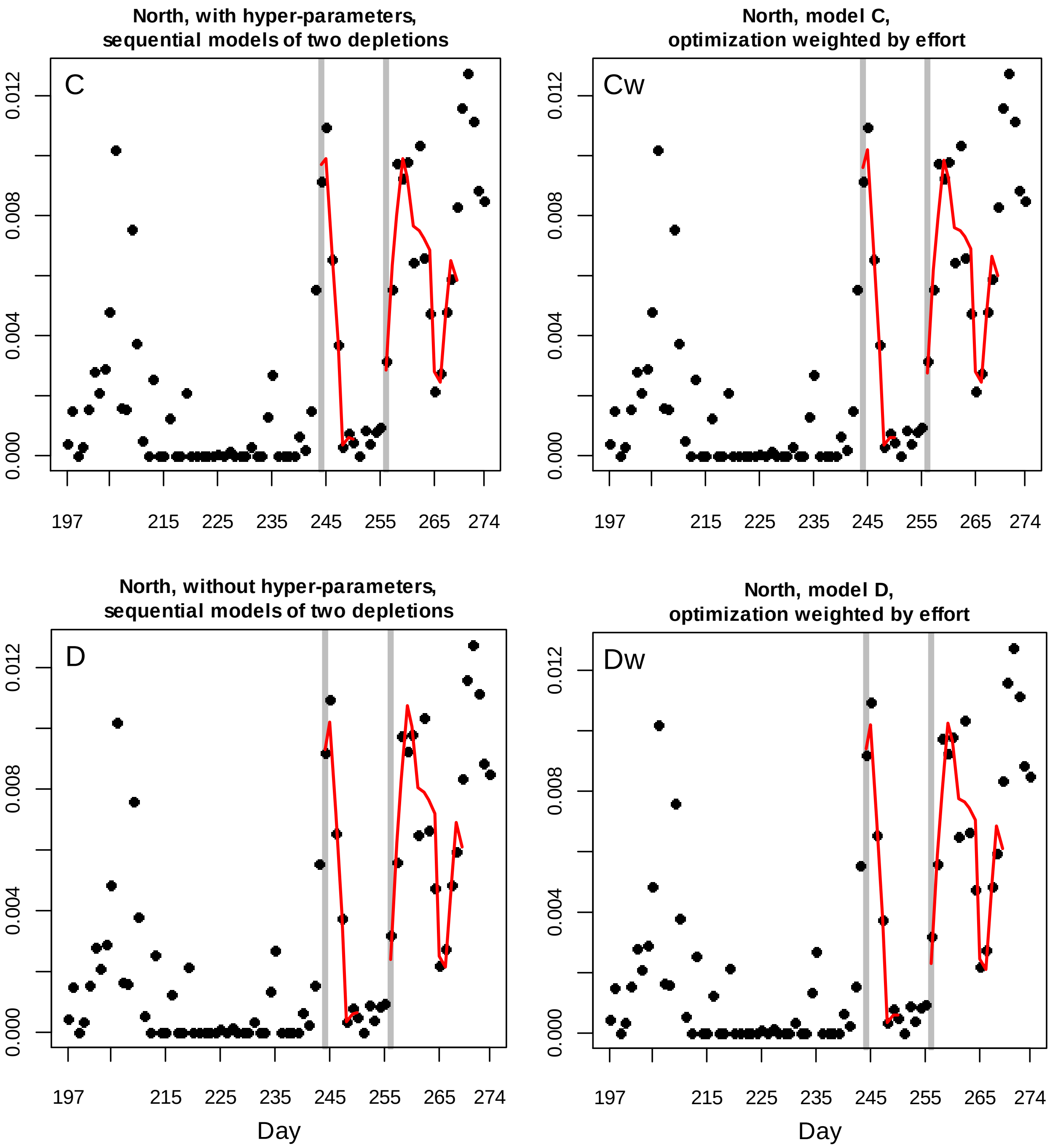


Figure A.3.1. Daily estimated catch numbers (black points) and expected catch numbers (red lines) projected from the north sub-area depletion periods starting on days 244 and 256, under four versions of the depletion model and variants with effort-weighted optimization.

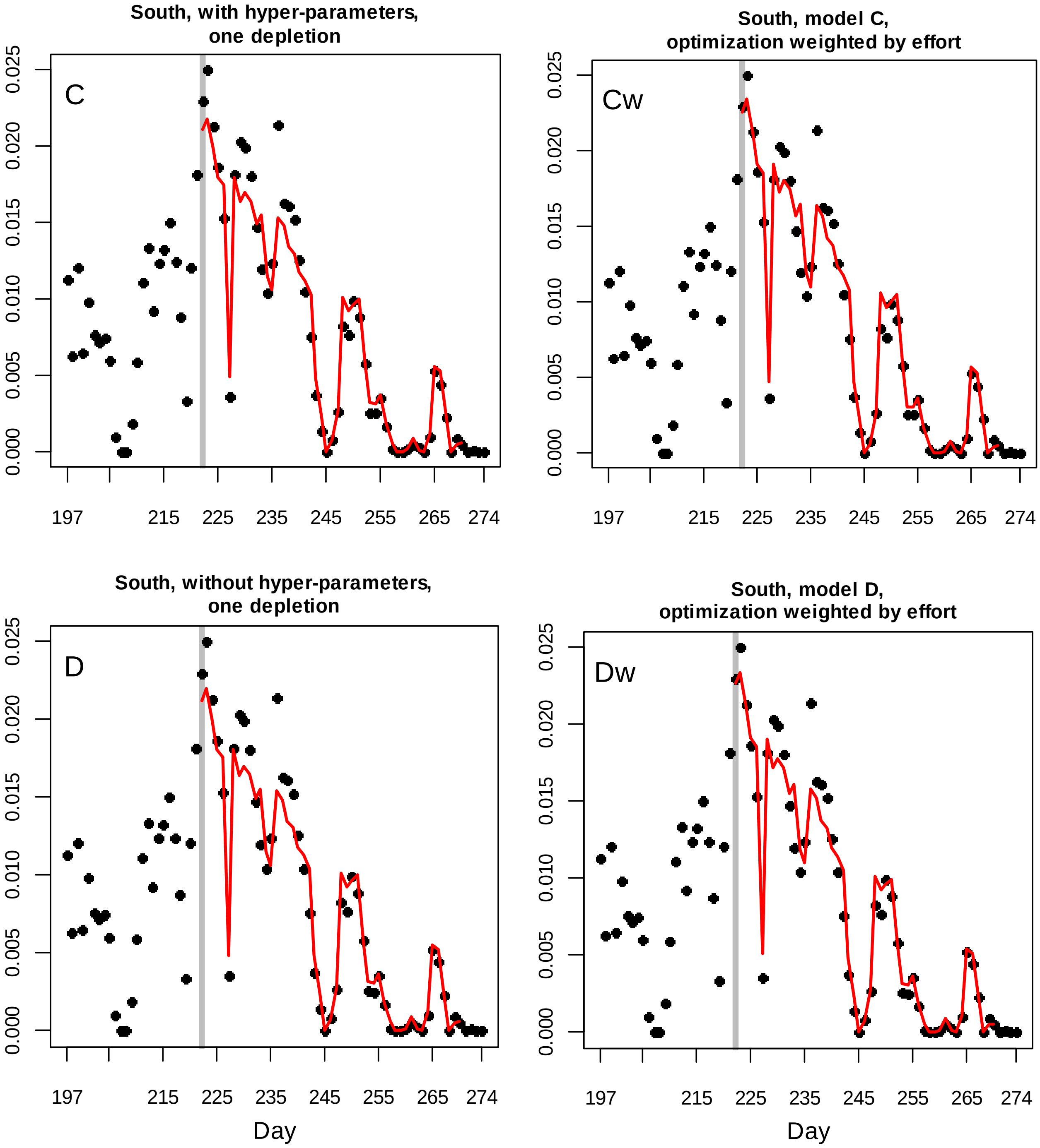


Figure A.3.2. Daily estimated catch numbers (black points) and expected catch numbers (red lines) projected from the south sub-area depletion period starting on day 222, under two versions of the depletion model and variants with effort-weighted optimization. (Versions A and B, as shown in Figure A.3.1, are irrelevant because there is only one depletion).

Table A1.1. Estimated numbers of *D. gahi*, root mean square errors (RMSE) of actual catch vs. predicted catch numbers, and catchability coefficients and hyper-parameters of the different versions of the depletion model (versions B and D don't fit hyper-parameters; the hyper-parameters are 1 by default). Refer to Figures A.3.1 and A.3.2 for description of the model versions. For versions C and D north, separate values are given for the first and second depletion periods.

| Sub-area | Model version | N (billions) | | RMSE | catchability coefficient | Hyper-parameters | |
|---|---|---|---|---|---|---|---|
| | | Start* | End* | | | Effort | Abundance |
| N | A | 0.06 | 0.04 | $1.14 \cdot 10^{-3}$ | $1.32 \cdot 10^{-3}$ | 1.020 | 0.312 |
| N | Aw | 0.09 | 0.07 | $1.14 \cdot 10^{-3}$ | $1.78 \cdot 10^{-3}$ | 1.036 | 0.512 |
| N | B | 0.22 | 0.20 | $1.12 \cdot 10^{-3}$ | $2.39 \cdot 10^{-3}$ | 1 | 1 |
| N | Bw | 0.21 | 0.17 | $1.12 \cdot 10^{-3}$ | $2.75 \cdot 10^{-3}$ | 1 | 1 |
| N | C | 0.29 | 0.24 | $0.82 \cdot 10^{-3}$ | $9.08 \cdot 10^{-1}$ | 0.962 | 5.568 |
| | | 0.32 | 0.19 | | $3.70 \cdot 10^{-3}$ | 0.832 | 1.010 |
| N | Cw | 0.04 | 0.01 | $0.81 \cdot 10^{-3}$ | $1.04 \cdot 10^{-2}$ | 0.876 | 0.699 |
| | | 0.31 | 0.19 | | $3.19 \cdot 10^{-3}$ | 0.849 | 0.926 |
| N | D | 0.06 | 0.02 | $0.87 \cdot 10^{-3}$ | $1.39 \cdot 10^{-2}$ | 1 | 1 |
| | | 0.30 | 0.17 | | $2.73 \cdot 10^{-3}$ | 1 | 1 |
| N | Dw | 0.05 | 0.02 | $0.83 \cdot 10^{-3}$ | $1.48 \cdot 10^{-2}$ | 1 | 1 |
| | | 0.34 | 0.21 | | $2.25 \cdot 10^{-3}$ | 1 | 1 |
| S | C | 1.13 | 0.34 | $1.11 \cdot 10^{-3}$ | $1.32 \cdot 10^{-3}$ | 0.985 | 0.869 |
| S | Cw | 1.12 | 0.33 | $0.97 \cdot 10^{-3}$ | $1.11 \cdot 10^{-3}$ | 1.069 | 0.888 |
| S | D | 1.41 | 0.48 | $1.08 \cdot 10^{-3}$ | $1.01 \cdot 10^{-3}$ | 1 | 1 |
| S | Dw | 1.21 | 0.38 | $0.98 \cdot 10^{-3}$ | $1.25 \cdot 10^{-3}$ | 1 | 1 |

* Of the depletion periods; not necessarily coincident with the entire season.

**(A.4)** Expected individual *D. gahi* weights calculated from generalized additive models (GAM) of the daily observer measurements and average vessel market size categories throughout the season.

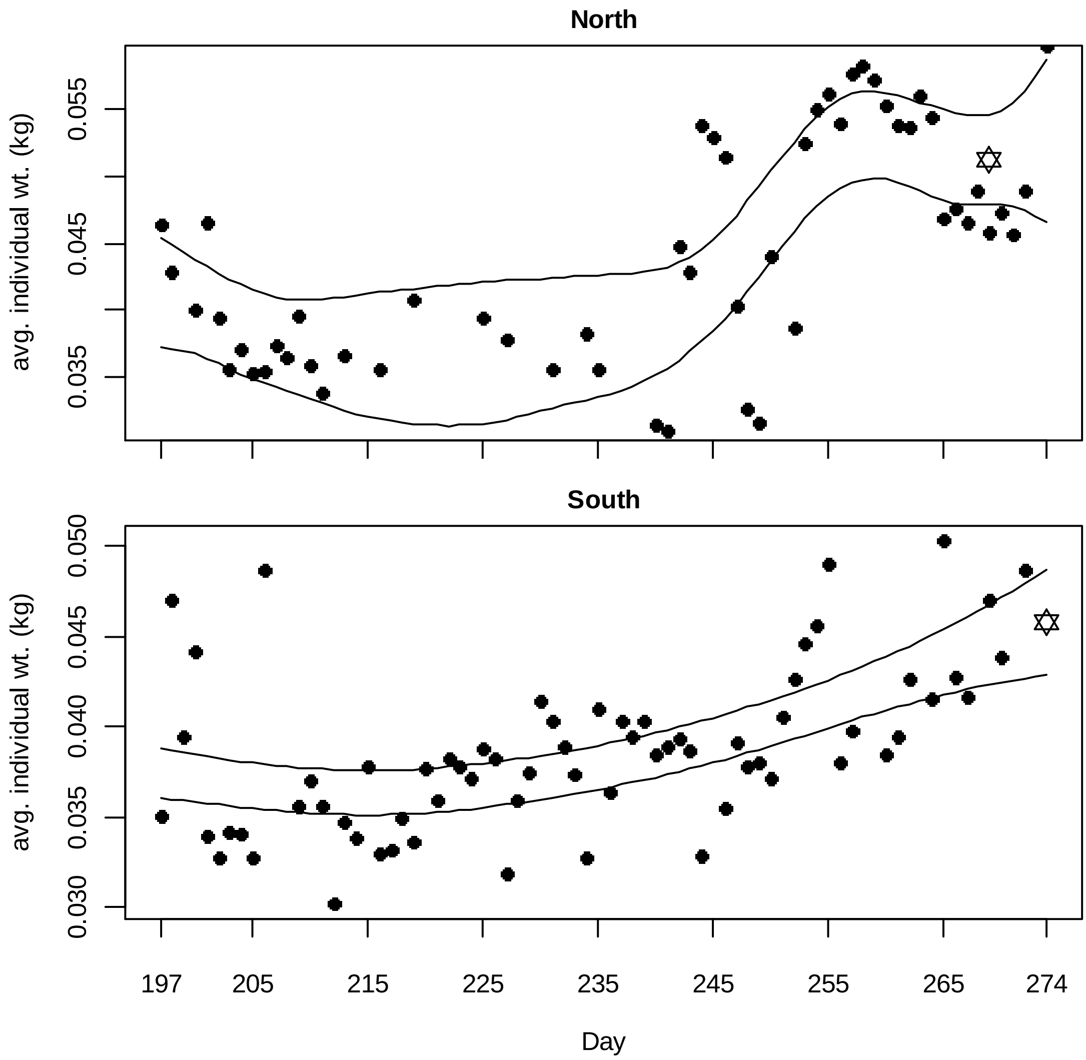


Figure A.4. Daily average *D. gahi* weights (black points) and 95% confidence intervals of GAMs (black lines) of seasonal trend in average individual weight. Star symbols indicate the expected average weights on the last depletion-modelled days: $Wt_{N\ day\ 269}$ = 51.3 g and $Wt_{S\ day\ 274}$ = 45.8 g.

(A.5) In-season immigration.

$$N_{N\ \text{immigration day 244}} = N1_{N\ \text{day 244}} - N_{N\ \text{survey day 244}}$$
$$= (0.224 \sim [0.150 - 1.001] - N(0.093, 0.037)) \times 10^9$$
$$= 0.132 \sim [0.044 - 0.914] \times 10^9$$
$$B_{N\ \text{immigration day 244}} = 0.132 \times 10^9 \times 41.1\ \text{g}$$
$$= 5406 \sim [1812 - 37764]\ \text{tonnes}$$
$$N_{N\ \text{immigration day 256}} = N2_{N\ \text{day 256}} - N_{N\ \text{survey day 244}}$$
$$= (0.167 \sim [0.117 - 0.636]) \times 10^9$$
$$B_{N\ \text{immigration day 256}} = 0.167 \times 10^9 \times 52.4\ \text{g}$$
$$= 8736 \sim [6099 - 33420]\ \text{tonnes}$$
$$N_{N\ \text{immigration day 270}} = N_{N\ \text{day 270 ratio}} - N_{N\ \text{day 270 depletion}}$$
$$= (0.201 \times 10^9\ [\text{equation } \mathbf{7}] \times 549.0 / 381.9) - 0.190 \times 10^9$$
$$= 0.099 \times 10^9$$
$$B_{N\ \text{immigration day 270}} = 0.099 \times 10^9 \times 51.4\ \text{g}$$
$$= 5076 \sim [942 - 37774]\ \text{tonnes}$$
$$N_{S\ \text{immigration day 222}} = N_{S\ \text{day 222}} - N_{S\ \text{survey day 222}}$$
$$= (1.133 \sim [0.798 - 3.629] - N(0.134, 0.050)) \times 10^9$$
$$= 0.999 \sim [0.654 - 3.500] \times 10^9$$
$$B_{S\ \text{immigration day 222}} = 0.999 \times 10^9 \times 36.6\ \text{g}$$
$$= 36516 \sim [23874 - 128027]\ \text{tonnes}$$
$$B_{\text{season total}} = B_{N\ \text{survey}} + B_{S\ \text{survey}} + B_{\text{immigration total}}$$
$$= 10838 \sim [8256 - 14885]$$
$$+ 18160 \sim [13456 - 23509]$$
$$+ 55735 \sim [32709 - 236992]$$
$$= 84733 \sim [54420 - 275392]$$